

Water soluble luminescent platinum terpyridine complexes with glycosylated acetylde and arylacetylde ligands: photoluminescent properties and cytotoxicities†

Dik-Lung Ma,^a Tina Yuen-Ting Shum,^a Fuyi Zhang,^a Chi-Ming Che^{*a} and Mengsu Yang^b

Received (in Cambridge, UK) 19th May 2005, Accepted 30th June 2005

First published as an Advance Article on the web 23rd August 2005

DOI: 10.1039/b507114c

Platinum(II) terpyridine complexes with glycosylated acetylde and arylacetylde ligands bind to DNA with binding constants $\sim 10^5 \text{ mol}^{-1} \text{ dm}^3$; the glycosylated arylacetylde complexes exhibit emission at $\lambda_{\text{max}} \approx 620 \text{ nm}$ in water and are up to ~ 100 -times higher in potency than the clinical cisplatin drug in killing cancer cells.

In the development of bioinorganic chemistry, the planar $[\text{Pt}(\text{terpy})\text{X}]^+$ complexes (terpy = 2,2':6',2''-terpyridine; X = Cl, SR) have frequently been cited as classic DNA metallointercalators.¹ However, application studies of $[\text{Pt}(\text{terpy})\text{X}]^+$ and their derivatives $[\text{Pt}(\text{terpy})\text{L}]^{n+}$ (L = monoanionic ligand, $n = 1$; L = neutral ligand, $n = 2$) in metal-based therapeutics remain sparse.^{2,3} The notable recent DNA study is by Lowe and co-workers who reported that platinum(II) complexes of 4'-substituted 2,2':6',2''-terpyridine exhibited cytotoxicity to *Trypanosoma* and *Leishmania* parasites as well as to human ovarian carcinoma.³ As noted in the literature, the chemistry of $[\text{Pt}(\text{terpy})\text{Cl}]^+$ under physiological conditions is easily complicated by its hydrolysis reaction, leading to aquation and/or substitution of the coordinated Cl^- .^{1a,b,e}

In this context, the $[\text{Pt}(\text{terpy})(\text{C}\equiv\text{C}-\text{Ar})]^+$ would be an appealing system for the following reasons: (i) $[\text{Pt}(\text{terpy})(\text{C}\equiv\text{C}-\text{Ar})]^+$ would resemble $[\text{Pt}(\text{terpy})\text{X}]^+$ as metallointercalator for biomolecules,¹ (ii) the strong Pt–C bond covalency would circumvent the problem of hydrolysis of $[\text{Pt}(\text{terpy})\text{Cl}]^+$, and (iii) the intriguing solvent/media dependence of the photoluminescence of $[\text{Pt}(\text{terpy})(\text{C}\equiv\text{C}-\text{Ar})]^+$ and related compounds⁴ suggests its potential applications in luminescent signalling studies of biological interest.⁵ We conceive that $[\text{Pt}(\text{terpy})(\text{glycosylated arylacetylde})]^+$ could be a new class of water soluble Pt^{II} complexes of potential biological interest. As the glycosylated substituent could be varied, it may be feasible to develop $[\text{Pt}(\text{terpy})(\text{glycosylated arylacetylde})]^+$ as luminescent probes for binding reactions of glycosylated biomolecules.

^aDepartment of Chemistry and Open Laboratory of Chemical Biology of the Institute of Molecular Technology for Drug Discovery and Synthesis, The University of Hong Kong, Pokfulam Road, Hong Kong.
E-mail: cmche@hku.hk; Fax: +852 2857-1586; Tel: +852 2859 2154

^bDepartment of Biology and Chemistry, City University of Hong Kong, 83 Tat Chee Avenue, Kowloon, Hong Kong

† Electronic supplementary information (ESI) available: experimental details; synthesis and characterisation of 1–7; UV/Vis absorption and emission spectra of 1–7 in Figs. S1–S5; restriction endonuclease fragmentation assay in Fig. S6; absorption titration spectra in Figs. S7–S9; emission titration spectra in Figs. S10–S11; flow cytometric analysis data in Fig. S12; cDNA microarray image in Fig. S13; photophysical data for 1–7 in Table S1; DNA binding data for 1–9 in Table S2; cDNA microarray data in Table S3. See <http://dx.doi.org/10.1039/b507114c>

The syntheses of the glycosylated ligands⁶ and their Pt^{II} complexes 1–7 (Chart 1) are given in the ESI.† Complexes 1–7 are soluble in both organic solvents (e.g. acetonitrile and dichloromethane) and water at room temperature. As revealed by both absorption and NMR spectroscopy, the Pt^{II}-glycosylated acetylde or arylacetylde moiety remains intact in aqueous solution for 72 h at room temperature.

The UV/Vis absorption spectra of 1–7 are given in the ESI† and the spectral data in H₂O are summarised in Table 1 (full spectral data are listed in the ESI†). With reference to previous studies,⁵ the absorption bands at 388–480 nm are assigned to metal-to-ligand charge transfer (MLCT) and ligand-to-ligand charge transfer (LLCT) transitions, which are solvent sensitive. Upon excitation at $\lambda > 380 \text{ nm}$, 1–7 in the solid state and in CH₂Cl₂ solution exhibit emission at 513–733 nm (see ESI†). Emission in H₂O solution was only observed for 1, 4 and 5 (see ESI†). Complexes 2, 3 and 6 which carry glycosylated acetylde but not arylacetylde ligand do not emit in H₂O solution.

Complexes 1–7 bind to DNA as revealed by restriction endonuclease fragmentation assay. Restriction endonucleases bind specifically to and cleave double-stranded DNA at specific sites within or adjacent to a particular sequence known as the recognition site. Once the DNA conformation is changed upon binding to a metal complex, restriction enzyme cannot recognise the DNA and no DNA cleavage would occur.⁷ The results of electrophoresis of the solutions after restriction enzyme digestion of pDR2 in the absence and presence of 1 are given in Supporting Information (see ESI†). Two bands corresponding to the supercoiled and nicked DNA were observed for the undigested DNA (Lane B). After ApaI digestion of pDR2, three bands corresponding to DNA fragments with 8, 5 and 2 kbp were obtained and resolved by agarose gel electrophoresis (Lane C). In the presence of the classical intercalator – ethidium bromide (4 μM), the minor groove binder – Hoechst 33342 (200 μM), or the intrastrand crosslinker – cisplatin (200 μM), DNA digestion was incomplete and bands attributed to the whole plasmid plus fragments were observed (Lanes D–F). Because 1 binds to DNA, treatment of pDR2 and ApaI with 1 at concentration 4 μM in 1 \times SuRE/Cut Buffer A inhibit the ApaI digestion and bands attributed to the whole plasmid plus fragments were observed (Lane G).

The binding to ct DNA was further examined by absorption titration. As an example, the absorption spectra of 6 treated with different concentrations of ct DNA in Tris buffered solution revealed spectral changes with hypochromism (15%) at 327 nm and only about 2 nm of bathochromic spectral shift (see ESI†). In contrast, the binding of $[\text{Pt}(\text{terpy})(\text{C}\equiv\text{C}-\text{C}_6\text{H}_5)](\text{CF}_3\text{SO}_3)$ (8) to DNA showed $\sim 40\%$ hypochromicity and $>10 \text{ nm}$ bathochromic

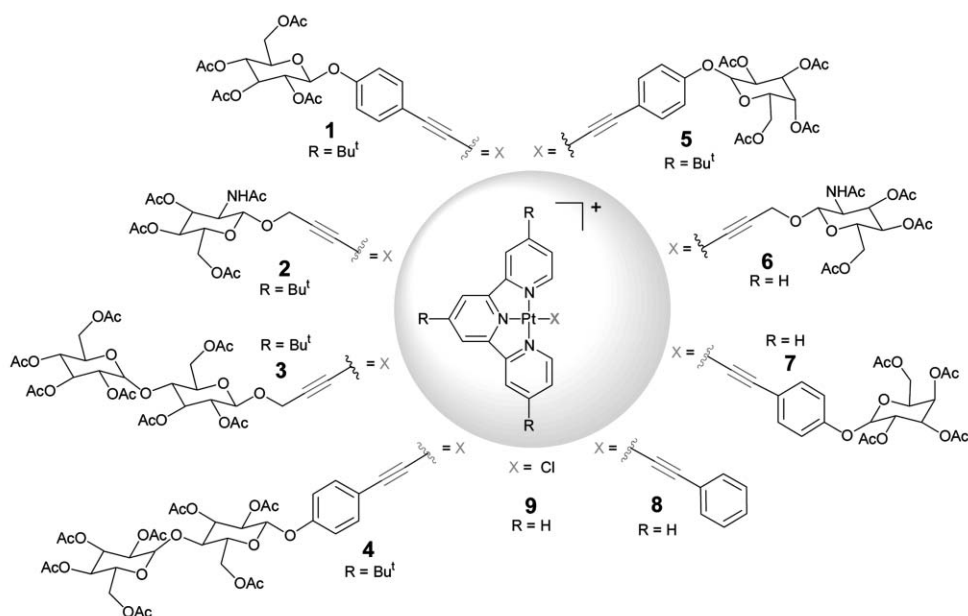


Chart 1 Schematic structures of $[\text{Pt}(\text{R}_3\text{terpy})\text{X}](\text{CF}_3\text{SO}_3)$ (**1–9**) with omission of the counteranions.

Table 1 Photophysical data for **1–7** in H_2O at 298 K

Complex	$\lambda_{\text{abs}}/\text{nm}$ ($\epsilon_{\text{max}} \times 10^{-3}/\text{dm}^3 \text{ mol}^{-1} \text{ cm}^{-1}$)	$\lambda_{\text{em}}/\text{nm}$ ($\tau/\mu\text{s}$)	$\phi_{\text{em}} \times 10^2$
1	326 (104.2), 341 (84.0), 450 (28.7)	619 (0.29)	3.7
1^a	314 (16.7), 339 (13.1), 412 (3.71), 470 (3.77)	615 (≤ 0.2) ^d	4.4
1^b	310 (32.5), 325 (31.1), 338 (31.5), 403 (8.90), 440 (9.30)	619 (≤ 0.2) ^d	0.052
1^c	311 (37.1), 325 (34.3), 339 (33.4), 404 (10.3), 440 (9.74)	624 (< 0.1)	0.048
2	318 (9.82), 382 (2.31)	non-emissive	
2^a	313 (10.2), 322 (8.88), 338 (9.85), 409 (2.30)	515 (0.23)	1.4
3	312 (11.8), 324 (118.7), 380 (2.73)	non-emissive	
4	324 (12.3), 450 (3.51)	621 (0.40)	1.2
5	314 (17.0), 324 (15.6), 340 (14.2), 411 (3.69), 470 (3.55)	623 (0.27)	1.4
6	328 (10.8), 342 (8.51), 388 (2.39)	non-emissive	
7	324 (14.0), 455 (5.20)	795 (< 0.1)	< 0.01

^a In CH_2Cl_2 . ^b In CH_3CN . ^c In CH_3OH . ^d Not single exponential decay.

shift (Fig. 1). A similar finding was observed with **9**. According to the literature, substantial hypochromism, extensive broadening and red shift of absorption band(s) are characteristic of intercalative interaction,⁸ as in the present case of **8**. Deriving from a plot of $D/\Delta\epsilon_{\text{ap}}$ vs. D according to the Scatchard equation (see ESI†),^{7b} the binding constant K at 20.0 °C was found to be $4.8 \times 10^5 \text{ mol}^{-1} \text{ dm}^3$ for **6**. The K values for **7–9** were similarly determined to be 3.7×10^5 , 6.9×10^5 and $3.9 \times 10^5 \text{ mol}^{-1} \text{ dm}^3$, respectively (see ESI†).

Complex **1** is weakly emissive in Tris buffered solution. However, in the presence of ct DNA, its emission at $\lambda_{\text{max}} = 619 \text{ nm}$ is enhanced, the intensity of which reaches a saturation level at $[\text{DNA}]/[\text{Pt}] \geq 3$ (see ESI†). As depicted by the plot of I/I_0 vs. $[\text{DNA}]/[\text{I}]$ (I and I_0 are emission intensities with and without DNA), less than 3-fold intensity enhancement was observed at $[\text{DNA}]/[\text{I}]$ ratio $\geq 3:1$ (see ESI†). For **7** which carries no ^tBu

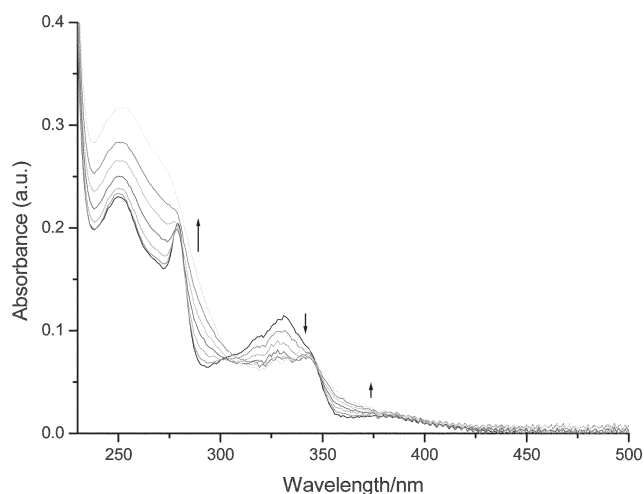


Fig. 1 UV/Vis spectra of **8** (50.0 μM) in Tris buffer solution with increasing ratio of $[\text{DNA}]/[\text{Pt}] = 0\text{--}1.00$ at 20.0 °C.

substituents in terpy ligand, the emission intensity increased up to 8-fold upon addition of ct DNA (see ESI†).

The binding mode to DNA was further examined by gel mobility shift assay (Fig. 2). For **1** which contains a bulky ^tBu₃terpy ligand, no significant change in DNA mobility was observed. This is typical of a groove binder as observed for Hoechst 33342. For **8**, which carries the planar terpy ligand, the DNA was lengthened and the DNA mobility was significantly reduced, and the extent of the mobility reduction was comparable to that found when the DNA solution was treated with the classical intercalator – ethidium bromide.⁹ Further analysis was also performed on **7**, which carries glycosylated arylacetylide ligand and the planar terpyridine, the DNA mobility was only slightly affected by increasing the concentration of **7**. We propose that the binding mode for **1** is groove binding. For **7**, both intercalation and minor groove binding modes could exist and a

Table 2 IC₅₀ values (μM) of 1–8 and cisplatin in five human carcinoma cell lines (HeLa, HepG2, SF-268, NCI-H460, MCF-7) and normal 293

Complex	HeLa	HepG2	SF-268	NCI-H460	MCF-7	293
1	0.1 ± 0.03	0.1 ± 0.01	0.06 ± 0.02	0.1 ± 0.03	0.08 ± 0.04	0.5 ± 0.1
2	17.8 ± 0.5	22.9 ± 0.8	17.1 ± 0.4	28.5 ± 1.9	17.1 ± 0.4	50.3 ± 7.2
3	2.0 ± 0.2	1.7 ± 0.1	1.3 ± 0.3	2.8 ± 0.6	1.9 ± 0.5	10.5 ± 0.4
4	0.09 ± 0.02	0.1 ± 0.02	0.08 ± 0.02	0.1 ± 0.01	0.1 ± 0.05	0.3 ± 0.08
5	0.2 ± 0.08	0.1 ± 0.05	0.1 ± 0.01	0.2 ± 0.09	0.2 ± 0.07	0.9 ± 0.1
6	19.2 ± 0.7	19.6 ± 1.6	15.1 ± 1.0	28.5 ± 2.5	15.4 ± 0.9	46.2 ± 5.3
7	0.2 ± 0.05	0.2 ± 0.08	0.1 ± 0.07	0.2 ± 0.06	0.1 ± 0.05	0.5 ± 0.4
8	2.7 ± 0.7	3.0 ± 1.1	2.1 ± 0.8	2.5 ± 0.8	3.4 ± 1.0	4.6 ± 1.2
Cisplatin	11.6 ± 0.2	20.6 ± 1.9	15.6 ± 0.2	25.1 ± 3.4	19.1 ± 1.7	>100

competing non-intercalative binding mode could reduce the extent of helix lengthening.

The cytotoxicities of 1–8 against five human carcinoma cell lines were measured by MTT assay, and the IC₅₀ values determined from the dose-dependence of surviving cells after exposure to the complexes for 48 h are listed in Table 2. All the Pt^{II}-glycosylated arylacetylde complexes show significantly higher cytotoxicities (IC₅₀ = 0.06–0.2 μM) against human cancer cells than cisplatin and the free ^tBu₃terpy, terpy, glycosylated acetylde and glycosylated arylacetylde ligands (IC₅₀ > 100 μM).

As depicted in Table 2, [Pt(terpy)(C≡C–C₆H₅)⁺] is at least 8-fold more cytotoxic than [Pt(terpy)Cl]⁺. Importantly, **1** is ~100 times higher in potency than the clinical cisplatin drug in killing cancer cells, and it is most cytotoxic among the reported [Pt^{II}-terpy] complexes.³ The glycosylated arylacetylde is apparently essential for the high cytotoxicities. Using human kidney cells (293) as model, **1** showed about 5 times higher cytotoxicity to cancer cells than to normal cells.

Based on cell morphology and cell membrane integrity, necrotic and apoptotic cells could be distinguished using flow cytometric analysis. **1** induced 52.3 ± 4.8% apoptosis selectively leading to cancer cell death and only 4.8 ± 1.4% necrosis was detected (see ESI†).

Treatment of NCI-H460 cells with **1** resulted in significant expression changes of 111 genes in comparison to untreated control cells (see ESI†). Analysis of the genes that were consistently and significantly regulated by **1** demonstrated significant **1**-dependent up-regulation of apoptosis related genes (C20orf97, PEA15, FN14 and PPM1F) and down-regulation of growth and cell cycle promoting genes (STK15, CRIP1 and PCNA). Preliminary microarray analysis was also performed on **8** and **9**, in order to examine gene induction events specific to the glycosylated substituent. To rule out nonspecific cellular responses to toxic insult, a 200-fold higher concentration of **9** was chosen for microarray comparison. Importantly, several of the genes such as C20orf97, PEA15, STK15 and PCNA with roles in cell proliferation and apoptosis that were significantly regulated by **1** became no longer differentially expressed after treatment of **8** or **9**.

In summary, the “Pt(terpy)(glycosylated arylacetylde)” system is cytotoxic in killing human cancer cells. The glycosylated arylacetylde is a key structure motif in governing the cytotoxicity, binding mode and cell death pathway.

This work is supported by the Area of Excellence Scheme established under the University Grants Committee of the Hong Kong Special Administrative Region, China (AoE/P-10/01) and The University of Hong Kong (University Development Fund).

A B C D E F G H I J

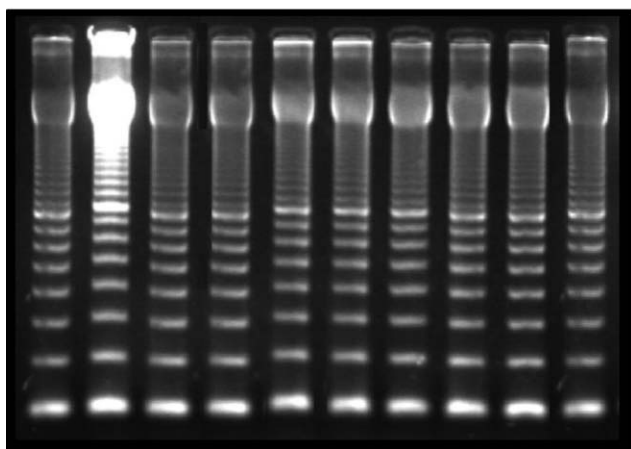


Fig. 2 Gel electrophoresis of a 100 bp DNA ladder in 2% (w/v) agarose gel showing the mobility of DNA. Lanes A and J are the 100 bp DNA. Lanes B and C are the 100 bp DNA in the presence of DNA interacting molecules: ethidium bromide (152 μM) (Lane B), Hoechst 33342 (152 μM) (Lane C). Lane D is the 100 bp DNA in the presence of **1** at 152 μM. Lanes E and F are the 100 bp DNA in the presence of **8** at 152 μM (Lane E) and 76 μM (Lane F). Lanes G–I are the 100 bp DNA in the presence of **7** at 152 μM (Lane G), 76 μM (Lane H) and 38 μM (Lane I).

Notes and references

- (a) K. W. Jennette, S. J. Lippard, G. A. Vassiliades and W. R. Bauer, *Proc. Natl. Acad. Sci. USA*, 1974, **71**, 3839; (b) M. H. Grant, K. C. Wu, W. R. Bauer and S. J. Lippard, *Biochemistry*, 1976, **15**, 4339; (c) L. P. Wakelin, W. D. McFadyen, A. Walpole and I. A. Roos, *Biochem. J.*, 1984, **222**, 203; (d) G. Arena, L. Monsù Scolaro, R. F. Pasternack and R. Romeo, *Inorg. Chem.*, 1995, **34**, 2994; (e) C. S. Peyratout, T. K. Aldridge, D. K. Crites and D. R. McMillin, *Inorg. Chem.*, 1995, **34**, 4484; (f) M. Cusumano, M. L. Di Pietro, A. Giannetto and F. Romano, *Inorg. Chem.*, 2000, **39**, 50.
- (a) S. J. Lippard, *Acc. Chem. Res.*, 1978, **11**, 211; (b) W. D. McFadyen, L. P. Wakelin, I. A. Roos and V. A. Leopold, *J. Med. Chem.*, 1985, **28**, 1113; (c) J. A. Todd and L. M. Rendina, *Inorg. Chem.*, 2002, **41**, 3331.
- (a) G. Lowe, A. S. Droz, T. Vilaivan, G. W. Weaver, J. J. Park, J. M. Pratt, L. Tweedale and L. R. Kelland, *J. Med. Chem.*, 1999, **42**, 3167; (b) G. Lowe, A. S. Droz, T. Vilaivan, G. W. Weaver, L. Tweedale, J. M. Pratt, P. Rock, V. Yardley and S. L. Croft, *J. Med. Chem.*, 1999, **42**, 999.
- W. Lu, B.-X. Mi, M. C. W. Chan, Z. Hui, C.-M. Che, N. Zhu and S.-T. Lee, *J. Am. Chem. Soc.*, 2004, **126**, 4958.
- (a) Q. Z. Yang, L. Z. Wu, Z. X. Wu, L. P. Zhang and C. H. Tung, *Inorg. Chem.*, 2002, **41**, 5653; (b) K. M.-C. Wong, W.-S. Tang, B. W.-K. Chu, N. Zhu and V. W. W. Yam, *Organometallics*, 2004, **23**, 3459.
- G. B. Giovenzana, L. Lay, D. Monti, G. Palmisano and L. Panza, *Tetrahedron*, 1999, **53**, 14123.
- (a) J. Sambrook, E. F. Fritsch and T. E. Maniatis, *Molecular Cloning, A Laboratory Manual*, 2nd edn, 1989, p. 5.31; (b) C. V. Kumar and E. H. Asuncion, *J. Am. Chem. Soc.*, 1993, **115**, 8547.
- W. I. Sundquist and S. J. Lippard, *Coord. Chem. Rev.*, 1990, **100**, 293.
- B. Åkerman, *J. Am. Chem. Soc.*, 1999, **121**, 7292.